Desalination and Water Treatment
www.deswater.com
doi: 10.5004/dwt.2021.27105

223 (2021) 299–315
May

Monolayer sorption capacity of copper(II), cadmium(II), and lead(II) from aqueous solution onto the surface of activated carbon prepared from *Terminalia catappa* leaf samples with reference to the calculation of thermodynamic parameters from Langmuir isotherm constant

Bandar R.M. Alsehli

Department of Chemistry, Faculty of Science, Taibah University, Al-Madinah Al-Munawarah 30002, Saudi Arabia, Tel. +966-552-055-010; email: bshle@taibahu.edu.sa

Received 10 August 2020; Accepted 6 February 2021

ABSTRACT

Polluted water that contains heavy metals, from industrial wastewater or other sources, has recently become a global concern, since most heavy metal varieties tend to accumulate in biota and have potentially poisonous impacts on different organisms. The specific objectives of this paper were: (1) to construct the sorption isotherm of metal ions (Cu^{2+}, Cd^{2+}, and Pb^{2+}) from a synthetic solution onto the surface of activated carbon (prepared from *Terminalia catappa* leaf samples), and (2) to determine the suitability of data fitting between the experimental and theoretical monolayer sorption capacity using Langmuir isotherm, (3) to calculate thermodynamic parameters based on Langmuir isotherm constant. The mixtures were incubated at (298 and 313 K) and shaken at 120 rpm for 3 h (equilibrium time). The Langmuir sorption isotherm demonstrated the correlation amongst the adsorbed amount on the surface (q_e) and the concentration that remained in the aqueous solution (C_e). The experimental adsorbed amount (q_e) for Cu^{2+}, Cd^{2+}, and Pb^{2+} at (298 and 313 K) reached (45.0 and 40.4 mg/g), (42.5 and 33.2 mg/g), and (27.5 and 24.0 mg/g), respectively. Thus, under comparable conditions, the ability of sorption increases in the order $Cu^{2+} > Cd^{2+} > Pb^{2+}$. The maximum monolayer sorption capacity Q_m at (298 and 313 K) was found to be: Cu^{2+} = (≈47 and 58 mg/g), Cd^{2+} = (≈45 and 44 mg/g), and Pb^{2+} = (≈29 and 26 mg/g). Thermodynamic parameters for heavy metal ions using Langmuir isotherm constant were calculated. All values of ($\Delta G°$, $\Delta H°$, and $\Delta S°$) were negative except the positive value of $\Delta S°$ for Pb^{2+}. The $\Delta S°$ and $\Delta H°$ are temperature independent. The negative numbers of $\Delta H°$ exemplify exothermic reaction. Negative $\Delta S°$, however, includes a less active interface of the liquid–solid system that causes sorption to be reduced. The negative value of $\Delta G°$ indicates the spontaneous sorption process.

Keywords: Inductively coupled plasma mass spectrometry; Heavy metals; Langmuir isotherm model; Aqueous solution; *Terminalia catappa*; Indian almond; Thermodynamic parameters

1. Introduction

Polluted water that contains heavy metals, from industrial wastewater or other sources, has recently become a global concern, since most heavy metal varieties tend to accumulate in biota and have potentially poisonous impacts on different organisms. Therefore, heavy metal contaminants must be treated and processed to ensure that alternate water source supplies are protected [1,2].

Sorption is a simple and uniform process for effective and low-cost treatment of heavy metals across different treatment technologies. Specific sorbents have been produced (synthetic and naturally derived materials) [3]. Madima et al. [4] demonstrated that the most economical

carbon-based adsorbents have been used in eliminating several organic and inorganic wastewater contaminants [2].

Both biochar and active carbon are pyrogenic carbonaceous materials (PCM). Their production comes from the thermochemical conversion of carbonaceous raw materials by activation or pyrolysis. The source of biochar is derived from sustainable biomass that is applied for non-oxidant utilization in agriculture, for example, in the soil. The sequestration of carbon is an atmospheric carbon dioxide's capture and storage process [5,6]. So, if biochar is applied as a fuel, for instance, by burning and oxidation to carbon dioxide, it is recognized as charcoal. Active carbon can be made from all sources of carbon (renewable, waste, or fossil), intended to be applied as a medium for the removal of gas and liquids pollutants [7,8].

Thus, it is classified as a strong adsorbent for pollutants with no requirements for the sustainability of its construction or carbon fate following its usage. Both activated carbon and biochar materials have a distinctive historical context, broadly divided research communities and independent literature bodies. Unfortunately, there is a general inconsistency in the accepted definition and terminology. Nevertheless, considering the similarity between the proposed applications for activated carbon and biochar, knowledge of the other domain could be valuable in either case. For instance, today soil remediation can be achieved by applying both activated carbon and biochar, which was previously merely an activated carbon's application [5,9]. If activated carbon is a sustainably-produced feedstock that meets further requirements [6,10], it can be called the biochar [11].

The initial definition of activated charcoal was any type of carbon that is cable of sorption [12]. The preparation of sorbent from charcoal has historically been dated in the past to the Chinese and Roman empires. The Roman empire started to realize that charcoal could clean up water, which is something, we still use. In spite of the long tradition of using charcoal to purify, it did take more than 3,000 y for humans to optimize charcoal for the elimination of toxic pollutants. In 1863, Smith [13] stated that oxygen was removed from the air by wood charcoal for a long time of more than a month. However, not every charcoal had the same capacity as wood charcoal had less sorption capacity than animal bone charcoal. This is where the work into similarities and features of charcoals contributing to specific sorption properties started to evolve rapidly. At the beginning of the 19th century, it was noticed that a number of organic compounds capable of sorption had also been noticed to be contained in charcoal [11,14]. The initial strategy of activation was to reduce adsorbed chemicals after production. Previously, the only method of removing charcoal was considered to be the thermal activation by Chaney [15]. The remains of the carbon skeleton and the exposition of pores and surface area were revealed. Hence, the chemical groups on the surface became activated for adsorption purposes. The activating carbon and charcoal science began with this.

In the 1920s, perhaps the first patents were granted for activating charcoal [16–18]. Though, the theoretical observations of increased sorption capacity were little theoretical grounding. Some of the leading works were empirical in large measure and focused on chemicals and various activation temperatures but lacked in a focused mechanism or hypothesis. The increase of sorption was generally presumed to be caused by new pores and perhaps surface area [19]. The activation in the 1950's was further defined as "any process that removes hydrogen or hydrogen-rich fractions in an open, pore residue selectively from a carbon-rich raw material" [20]. Key elements of activation are still the chemical and structural changes that contribute to the increase in surface's area and adaptive alterations of specific chemical moieties. Total porosity, mechanical strength, diffusivity, and surface load are also important [11,21].

Theoretical studies of charcoal activation and related bromine adsorption were started by Wright [22]. Before and after activation comparable sorption of bromine power was remarked. After thermal activation, the mechanism of bromine sorption had changed, from anion substitution to chemical additional carbon reactions. The activation theorized the existence of unsaturated C-bonds. In 1930, Lowry [23] concentrated on this process and found that the potential sorption or removal of active charcoal is linked to the overall content of hydrogen and non-aromatic existence/unsaturated carbon bonds. Ruff and Schmidt [24] presented evidence with the advent of modern methods to analyze crystalline structure, showing that there are no improvements in the physical structure other than surface chemistry. There was no semi-continuous character of the sheets of graphite, also isolated graphite and active charcoal fragments had been found [11].

Detection of sorption pathways is hampered by many complicating factors. The first consideration is that under extreme conditions charcoal is changed. After storage under laboratory conditions, Shelton [25] in 1920, recorded a triple shift in N_2 sorption capacity. A second factor is a contribution to the sorting processes on the charcoal by precipitated inorganic salts (ash content) [11].

Activated carbon, apart from potential sorption, may as well behave as a catalyst, for example in the anaerobic azo dyes' reduction, besides promotes radical development in the treatment of industrial effluent by oxidizer dyes and/or contaminants [11,26,27], and is utilized in a microbial fuel cell (MFC).

The global demand for activated carbon increases with several markets. The new law establishes standards for purification of mercury emissions from electrical power plants, among others, for energy storage systems, drinking water, and for the environment [28]. The annual net carbon market value of $3.0 billion (USD) was estimated [29]. In 2015, powdered activated carbon represented about 50% of the overall market for activated charcoal [29]. Granular activated carbon (GAC) accounted for about 30% of the overall demand (VOC and chlorine removal) with the remaining 20% of the polymer-coated, extruded, and impregnated-activated carbons [11,29].

Activated carbon surface has its own uniqueness. The structure is porous and defines sorption capacity, the chemical structure affects the interactions with non-polar and polar adsorbates. The activated sites are in the type of displacements and edges, which define the chemical reactions among most of the atoms. Therefore, an activated carbon's sorption behavior could not be interpreted solely on the pore size and surface area distribution. Activated

carbons with the same surface area but handled by various procedures or various activation strategies have significantly different sorption characteristics. Consequently, a complex chemical structure must be calculated by deciding the right sorption model. The appropriate model should consider the chemical structure and porosity of the activated carbon that incorporates the concentration, chemical groups, surface area, surface polarity, distribution of pore size, along with the chemical and physical properties of the adsorbate (i.e., molecular dimensions, polarity, etc.). The solution concentration and pH are essential added elements in the sorption from solutions. Therefore, activated carbons are very flexible and excellent adsorbents [30].

Their important uses include the removal of odor, colors, and tastes; treatment of toxic wastewaters and other undesirable drinking water, inorganic, and organic contaminants; for the purification of a wide variety of chemicals, foodstuffs, and pharmaceutical wastes. Its use in medicine and health applications is being rapidly developed for blood purification to tackle various forms of bacteria and remove specific poisons and toxins [30].

It is possible to use activated carbons in different forms: the granulated activated carbons (GACs), powdered activated carbons (PACs), and the fibrous activated carbon fibers (ACFs). PACs typically have smaller particle sizes of about 44.0 μm that allow quicker sorption although they are hard to manage in fixed sorption beds. Moreover, they may lead to a high drop in pressure that are challenging to re-generate. GACs are abrasion resistant and have granules about 4.0–0.6 mm in size and considerably dense to sustain operational requirements. Though they are more costly than PACs, they can be conveniently regenerated as they cause low hydrodynamic resistance. GACs that are applied in a certain module formulation could be re-generated after heat saturation on steam. ACFs are not cost-effective wastewater treatment's materials but they can simply fit into the sorption system and produce low hydrodynamic flow resistance [30].

The research presented in this paper aims to evaluate the efficiency of the sorption of Cu^{2+}, Cd^{2+}, and Pb^{2+} from aqueous-solid solution using activated carbon (prepared from *Terminalia catappa* leaf samples). The specific objectives of this paper were: (1) to construct the sorption isotherm of metal ions (Cu^{2+}, Cd^{2+}, and Pb^{2+}) from a synthetic solution onto the surface of prepared activated carbon, and (2) to determine the suitability of data fitting between the experimental and theoretical monolayer sorption capacity using Langmuir isotherm, (3) to calculate thermodynamic parameters based on Langmuir isotherm constant.

2. Materials and methods

2.1. Materials and chemicals

Adsorbent: *T. catappa* leaf samples (traditionally known as Indian almonds) were thoroughly rinsed with deionized water to get rid of dirt and suspended matter. Then samples were oven-dried at 70°C for 48 h. The oven-dried leaves were mixed with concentrated H_2SO_4 at 100°C for 24h and then neutralized with $NaHCO_3$ solution, rinsed extensively with deionized water, and oven-dried at 70°C for 48 h. Eventually, the synthesized biomass from Indian almond leaves was crushed then sieved at a uniform size of 300 μm. This procedure for preparation of biomass adsorbent was adapted from Parajuli et al. [31]. The prepared adsorbent materials were stored in airtight bottles to be used in this study.

Adsorbate stock solution in deionized water: element standards (1,000 mg/L) for Cu^{2+}, Cd^{2+}, and Pb^{2+} were prepared from $Cu(NO_3)_2{\cdot}3H_2O$, $Cd(NO_3)_2{\cdot}4H_2O$, and $Pb(NO_3)_2$ (purity ≥ 99%, Sigma-Aldrich, UK), respectively. Working concentrations were prepared by serial dilution in deionized water. These salts are very soluble in aqueous solutions.

The shaker and incubator (model ZWY-100H, no. CE ISO9001, 433DDA19) were applied to all sorption studies. Filtration of the aqueous solution was done by first washing the syringe filter (Acrodisc®nylon, 25 mm diameter, 0.45 μm pore size,) with the same sample and then the filtrates were analyzed by inductively coupled plasma mass spectrometry (ICP-MS; Agilent ICP-MS 7500, UK Cheshire, SK8 3GR). The instrument was tuned and calibrated.

2.2. Equilibrium time

A fixed amount of 0.1 g from adsorbent was mixed with 50 mL of 80 mg/L concentration of heavy metal in 120 mL screw caps bottles. The solution was maintained at pH ≈ 6 and the mixtures were incubated at two different temperatures (298 and 313 K) and shaken at 120 rpm for 10–350 min. At each time interval, a small aliquot was taken and filtered. The adsorption (%) was determined by ICP-MS according to Eq. (1):

$$\text{Adsorption}\,(\%) = \frac{\left(C_0 - C_e\right)}{C_0} \times 100 \tag{1}$$

2.3. Kinetic studies

To evaluate the sorption rate for cations (Cu^{2+}, Cd^{2+}, and Pb^{2+}) onto the adsorbent, pseudo-first-order rate and pseudo-second-order rate models were tested to fit the kinetic data (see result and discussion section).

2.4. Sorption isotherm

Sorption isotherm experimentations were set by batch experiments in which a fixed amount of 0.1 g from adsorbent was mixed with 50 mL of different concentrations of heavy metal in 120 mL screw caps bottles. The solution was maintained at pH ≈ 6 and the mixtures were incubated at two different temperatures (298 and 313 K) and shaken at 120 rpm for 3 h (equilibrium time). After that, the solutions were filtered, and the adsorbed amounts were determined by ICP-MS according to Eq. (2):

$$\text{Adsorbed amount}\; q_e(\text{mg/g}) = \frac{\left(C_0 - C_e\right)}{W} \times V \tag{2}$$

where C_0 is the initial metal ions concentration (mg/L), C_e is the final concentrations (mg/L), V is the volume of metal ion solution (50 mL), and W is the adsorbent weight (g).

The amount adsorbed q_e (μg/g) was divided by 1,000 to express it as mg/g.

2.5. Langmuir isotherm and the monolayer sorption capacity

The isotherm model of Langmuir is employed to define the equilibrium between the system of adsorbent and adsorbate, where the sorption is confined to a single layer at or prior to a relative pressure. While this isotherm originally introduced by Langmuir in 1918 is perfectly adequate for illustrating the process of chemisorption whenever covalent or ionic bonds form between the adsorbate and the adsorbent. The formula has adhered to a lot of processes with relatively low coverage and it could be clearly expanded to portray the action of the binary sorption. Additionally, Langmuir states that the surface fractional coverage θ is directly proportional to the surface desorption rate, the equilibrium desorption, and sorption rates.

$$k_a C_e \left(1-\theta\right) = k_d \theta \tag{3}$$

where k_a is the corresponding sorption rate constant; k_d is the corresponding desorption rate constant.

The additional common type of the formula is defined:

$$\theta = \frac{q}{q_e} = \frac{bC_e}{\left(1+bC_e\right)} \tag{4}$$

$$b = \frac{k_a}{k_d} \tag{5}$$

where C_e is the equilibrium concentration of adsorbate in the aqueous phase (mg/L); q_e is the adsorbate amount that adsorbed in a single monolayer (mg/g); b is a constant associated with the free energy of sorption and the reciprocal concentration with which half the adsorbent saturation is achieved. It is also called the Langmuir isotherm equilibrium constant (L/mg).

The sorption isotherm model of Langmuir particularly defines the homogeneous surface, meaning that there is no adjacent contact between adjacent adsorbed molecules when one single molecule occupies a single surface location. The Langmuir equations are a combination of nonlinearization and linearization which is described in Eqs. (6) and (7):

Nonlinear form:

$$q_e = \frac{Q_m b C_e}{1+bC_e} \tag{6}$$

Linear form:

$$\frac{C_e}{q_e} = \frac{1}{bQ_m} + \frac{C_e}{Q_m} \tag{7}$$

where Q_m is the monolayer sorption capacity (mg/g).

The key characteristic of the Langmuir isotherm can be described by a dimensionless constant R_L, which is called the separation factor or equilibrium parameter, defined by Eq. (8):

$$R_L = \frac{1}{1+bC_0} \tag{8}$$

where C_0 is the adsorbate's initial concentration. The form of the isotherm could be suggested via the R_L value. It is linear when (R_L = 1), unfavorable (R_L > 1), irreversible (R_L = 0), and favorable when $0 < R_L < 1$.

Table 1
Equations of Freundlich, Temkin, and Dubinin–Radushkevich isotherm models

Isotherm model	Nonlinear form	Linear form	No.
Freundlich	$q_e = K_F C_e^{1/n}$	$q_e = \log K_F + \frac{1}{n}\log C_e$	(9)
Temkin	$q_e = \frac{RT}{b_T}\ln A_T C_e$	$q_e = \left(\frac{RT}{b_T}\right)\ln A_T + \left(\frac{RT}{b_T}\right)\ln C_e$ $B = \frac{RT}{b_T}$	(10)
Dubinin–Radushkevich	$q_e = \left(q_s\right)\exp\left(-k_{\text{ad}}\varepsilon^2\right)$	$\ln\left(q_e\right) = \ln\left(q_s\right) - k_{\text{ad}}\varepsilon^2$ $E = \left[\frac{1}{\sqrt{2B_{\text{DR}}}}\right]$ $\varepsilon = RT\ln\left[1+\frac{1}{C_e}\right]$	(11)

where Freundlich parameters: K_F (mg/g): Freundlich isotherm constant, n: constant of sorption intensity; Temkin parameters: T: temperature at 298 and 313 K; R: constant of universal gas (8.314 J/mol K); A_T: Temkin's binding equilibrium constant (L/g); B: sorption heat constant (J/mol); b_T: Temkin's isotherm constant.

Dubinin–Radushkevich parameters: q_s: D-R saturation capacity (mg/g); q_e: adsorbate amount at equilibrium (mg/g); E: mean of free energy (kJ/mol); k_{ad}: constant of D-R isotherm (mol²/kJ²); ε: D–R isotherm constant; B_{DR}: D–R isotherm constant.

2.6. Freundlich, Temkin, and Dubinin–Radushkevich isotherms and the multilayer sorption

These models consider the multilayer sorption process in heterogenous surface. More detailed descriptions about the theory and application of these isotherms can be found in our previous published paper [32]. Table 1 summarizes the equations for each isotherm model.

2.7. Thermodynamic parameters from the constant (b) of Langmuir isotherm

The parameters of the thermodynamic process, that is, change in standard entropy ($\Delta S°$), change in standard enthalpy ($\Delta H°$), and Gibbs free surface energy change ($\Delta G°$) characterize the viability of the process of sorption. For evaluating these parameters, the van't Hoff equation has been extensively used. The key requirement in the sorption process is the equilibrium constant. The equation constant of van't Hoff was calculated by different considerations, including the Freundlich model isotherm constant, the distribution coefficient, and other approaches [33–40]. Langmuir isotherms were commonly used along with or without modification [41–45]. The major difference region in this field is a clear lack of continuity and variation in the determination of the constant of thermodynamic equilibrium. Moreover, the unitless equilibrium constant according to thermodynamics reaction needs to be calculated by $\Delta G°$. Its implications would be obviously refuted by the significant application of a Langmuir isotherm constant with a unit of (L/g), (L/mg), or (L/mol), etc. To evaluate the sorption thermodynamics parameters, a single formula for the derivation of van't Hoff constant is needed [46]. The thermodynamic parameter has usually been determined as follows from van't Hoff's Eq. (12):

$$\ln K_{eq} = -\frac{\Delta H°}{RT} + \frac{\Delta S°}{R} \tag{12}$$

where K_{eq} is the equilibrium constant; T is the temperature (K); R is the universal gas constant (0.008314 kJ/mol/K).

Generally, the $\Delta H°$ and $\Delta S°$ can be obtained by plotting $\ln K_{eq}$ against $1/T$. The slope and intercept then multiplied by R. The $\Delta G°$ can be calculated from any of the following Eqs. (13) and (14):

$$\Delta G° = \Delta H° - T\Delta S° \tag{13}$$

$$\Delta G° = -RT\ln K_{eq} \tag{14}$$

There are some notes that need to be added to these equations which will be discussed in the result and discussion section.

3. Results and discussion

3.1. Equilibrium time

The results to determine the sorption of cations (Cu^{2+}, Cd^{2+}, and Pb^{2+}) onto the activated carbon of *T. catappa* leaf samples as a function of time are shown in Fig. 1.

The pattern suggested that the sorption process on the surface is heterogeneous with fast sorption at an initial time and a slower rate close to the plateau of the curve. The initial process of rapid adsorption could be a result of ion-exchange on the surface of the activated carbon's micropores. Conversely, slower sorption after the initial phase could be attributed to weaker diffusion of cations into the activated carbon interior channels. The sorption% for Cu^{2+}, Cd^{2+}, and Pb^{2+} at 298 and 313 K reached 85% and 65%, 78% and 65%, and 70% and 63%, respectively. The equilibrium time was 180 min.

Some literature reviews [30,47] have shown that the most critical factors that affect and assess the metal ions sorption into aqueous-solid solutions are the functional carbon–oxygen groups on the activated carbon surface and the solution's pH. The ionic and molecular species nature and concentration in the solution are determined by these two parameters. Several electrokinetic experiments have shown that increasing or decreasing the pH of the activated carbon-solution system will alter the concentration and structure of the carbon surface charge.

The activated carbon's surface is charged positive below the zero-point charge (pHzpc) and charged negative above ZPC. The activated carbon surface is positively charged when it contains basic groups that are excessively protonated at low values of pH. In addition, sorption from aqueous solutions is enhanced by the formation of acceptor–donor complexes due to the existence of graphene layers (play an important role as Lewis bases) [30].

In this study, screening experiments related to the pH effect (figure is not shown) suggested that pH 6 was optimum to carry sorption study. At higher pH and because of ionizing of acidic carbon–oxygen groups, the activated carbon surface has a negative charge. The sorption of metal ions therefore typically involves repulsive and attractive electrostatic interactions among the solution of ionic species and negative sites formed by acidic groups ionization on the activated carbon's surface. The dispersed interactions between the ionic particles, surface, and graph layers of the solution contribute very little to inorganic sorption. Nevertheless, the case is different in the sorption of organic compounds. The organic compounds in water could be nonpolar or polar and play an important role not merely in electrostatic interactions but comparably in dispersive interactions [30].

A microcrystalline structure of activated carbon continues building up in the process of carbonization. Though, the microcrystalline structure of active carbon varies from graphite in the inter-layer spacing, which is 0.335 nm for graphite and 0.34–0.35 nm for active carbons. The microcrystalline layer coordination is also different, as active carbons are less ordered. The phrase *turbostratic* for such a structure was suggested by Biscoe and Warren [48]. The presence of heteroatoms such as hydrogen, oxygen, and deficits like vacant lattices in active carbon causes this disorder on microcrystalline layers.

3.2. Kinetic studies

To evaluate the sorption rate for cations (Cu^{2+}, Cd^{2+}, and Pb^{2+}) onto the adsorbent, pseudo-first-order rate and

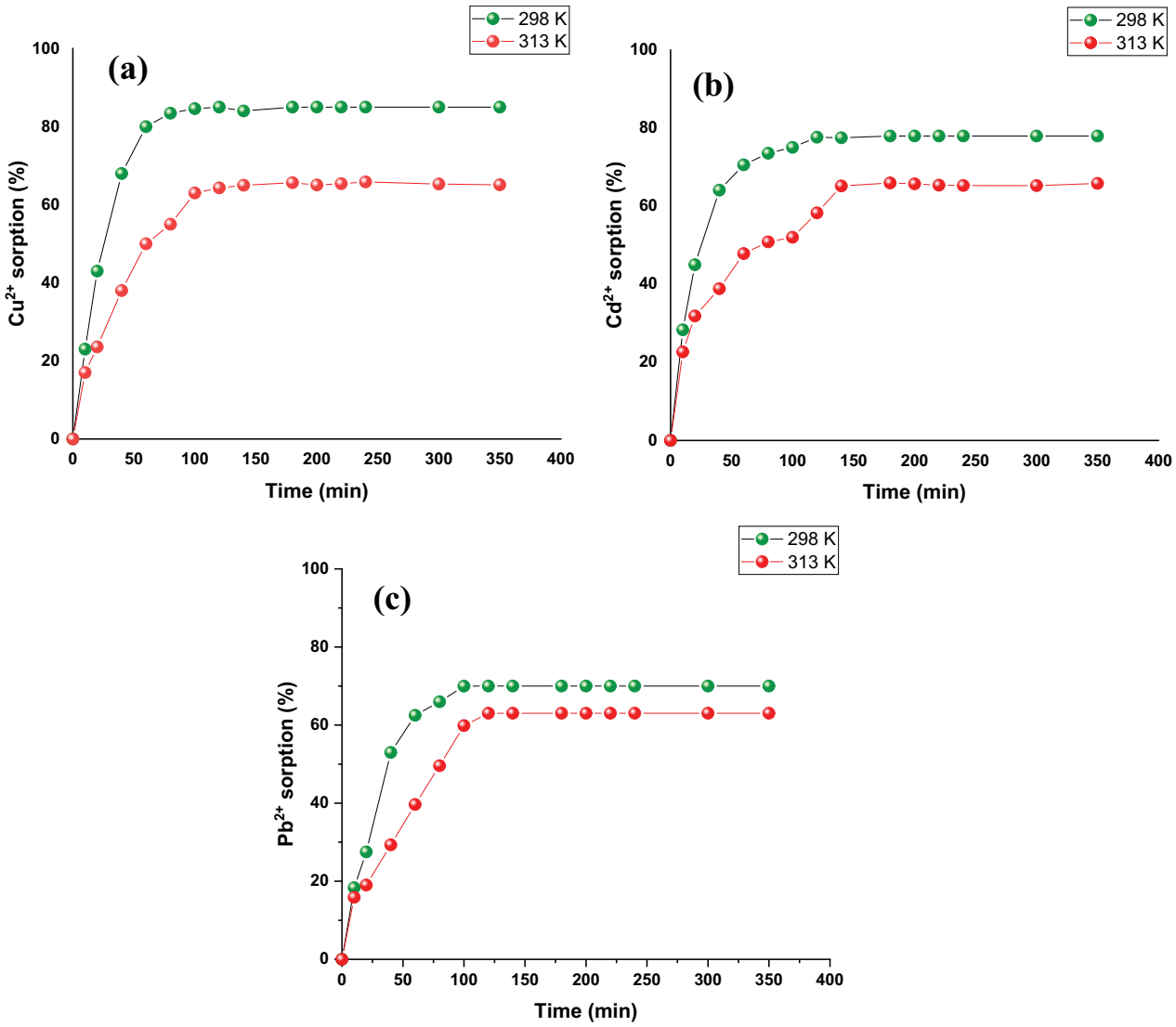

Fig. 1. Kinetics study of (a) Cu^{2+}, (b) Cd^{2+}, and (c) Pb^{2+} at 298 and 313 K, pH 6.

pseudo-second-order rate models were tested to fit the kinetic data. The kinetics equations are as follows:

Pseudo-first-order [49]

$$\ln\left(q_e - q_t\right) = \ln q_e - K_1 \times t \tag{15}$$

where q_e, q_t, and K_1 are the amounts adsorbed at equilibrium (mg/g), the amount adsorbed at time t (mg/g), and the rate constant of pseudo-first-order (min^{-1}), respectively.

Pseudo-second-order [50]:

$$\frac{t}{q_t} = \frac{1}{K_2 \times q_e^2} + \frac{t}{q_e} \tag{16}$$

where K_2 (g/mg min) is the rate constant of pseudo-second-order.

The values of q_e, K_1, and K_2 can be determined from the slope and intercept of the model plot. Fig. 2 shows the lineal graphics of the kinetic models at 298 and 313 K.

The calculated values of maximum adsorption capacities q_e, K_1, K_2, and R^2 values obtained for kinetics models are displayed in Table 2. The values of R^2 for Cu^{2+} and Pb^{2+} adsorption fit better for the pseudo-first-order model while Cd^{2+} adsorption fits for the pseudo-second-order model. In general, the values of K_1 and K_2 were higher with increasing temperature (except Cd^{2+}) indicating cations heterogeneous adsorption. The Cu^{2+} resulted in a value of K_1 higher than Pb^{2+}. The order of adsorption capacities was $Cu^{2+} > Cd^{2+} > Pb^{2+}$.

The adsorption results of the cations showed different kinetic orders, suggested that the adsorption surface was energic heterogeneous, and electrostatic attraction and the presence of solvent species influenced the mechanism of adsorption of these soft cations on surface basic groups.

3.3. Sorption isotherm

Figs. 3a–c show sorption isotherms for metal ions at 298 and 313 K. The isotherms demonstrated the relation

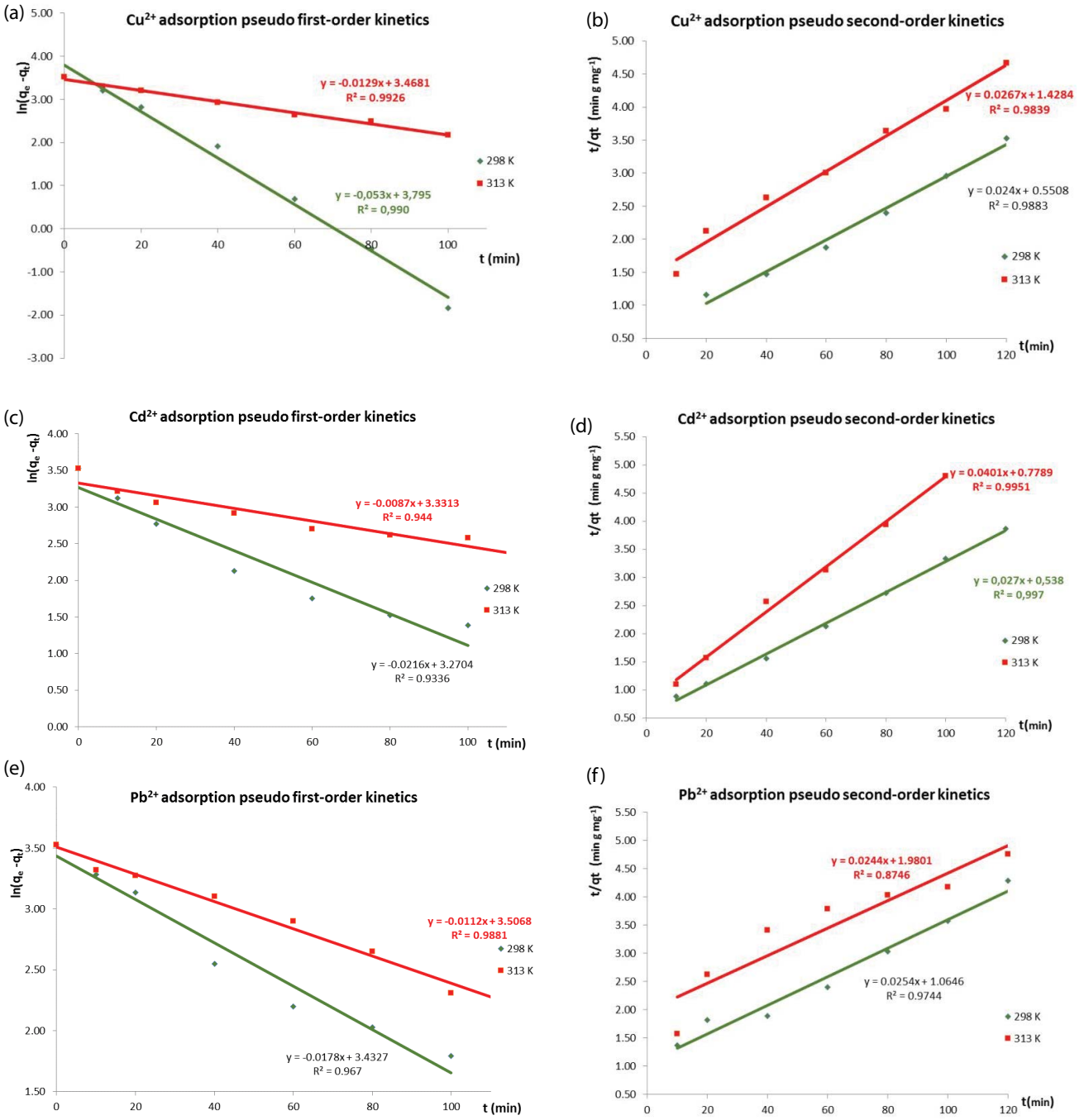

Fig. 2. Pseudo-first-order and pseudo-second-order adsorption kinetics of (a) Cu^{2+}, (b) Cd^{2+}, and (c) Pb^{2+} at 298 and 313 K, pH 6.

between the amount adsorbed on the surface (q_e) and the remained concentration in the solution (C_e). The experimental adsorbed amount (q_e) for Cu^{2+}, Cd^{2+}, and Pb^{2+} at (298 and 313 K) reached (45.0 and 40.4 mg/g), (42.5 and 33.2 mg/g), and (27.5 and 24.0 mg/g), respectively. Thus, under comparable conditions, the ability of sorption increases in the order $Cu^{2+} > Cd^{2+} > Pb^{2+}$.

The goodness of the fit through these experimental points was left without scattering lines as these lines might introduce some errors and do not predict the correct link between the points. Langmuir isotherm Eqs. (6) and (7) were used in the next section to mimic the behavior and propose a suitable theoretical line.

Many investigations [51–58] have been carried out on the applicability of active carbon in the sorption of inorganics. There are two factors to the sorption of inorganic compounds: eliminating contaminants and extracting other metals for instance silver and gold. In addition, the activated carbon packing with other metals creates impregnated metal-active carbon that is quite beneficial for the

Table 2
The correlation parameters of the kinetics models

Adsorbate	Correlation parameters for adsorption kinetics						
	Pseudo-first-order				Pseudo-second-order		
	T (K)	$K_1 \times 10^2$ (min^{-1})	q_e (mg/g)	R^2	$K_2 \times 10^2$ (g/mg min)	q_e (mg/g)	R^2
Cu^{2+}	298	5.39	44.5	0.990	0.1047	41.6	0.988
	313	1.29	32.1	0.992	0.0488	37.9	0.983
Cd^{2+}	298	2.16	26.3	0.933	0.1377	36.7	0.997
	313	0.88	28.0	0.944	0.2068	24.9	0.995
Pb^{2+}	298	1.78	31.0	0.967	0.0604	39.4	0.974
	313	1.12	33.4	0.988	0.0301	40.9	0.874

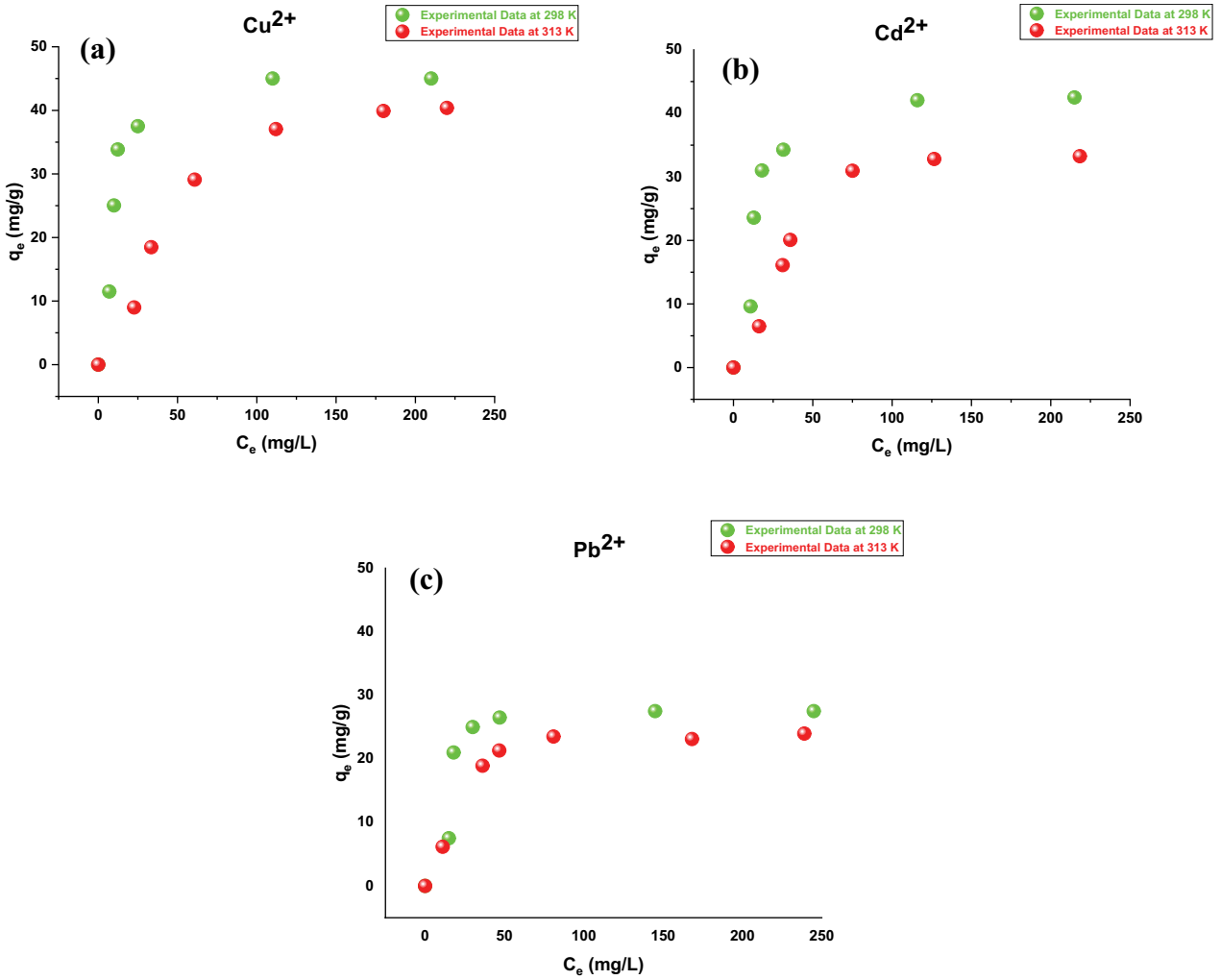

Fig. 3. Experimental sorption isotherms for (a) Cu^{2+}, (b) Cd^{2+}, and (c) Pb^{2+} at 298 and 313 K.

catalytic breakdown of gasses in sewage and for the defense against noxious war gasses such as $COCl_2$, HCN, $CNCl_2$, or nerve gases.

Active carbons have an ability to adsorb inorganic compounds, in particular metal cations, because of their characteristics of ion exchange owing to the existence of other heteroatoms such as sulfur, halogens, oxygen, and nitrogen. They are bound to the surface of carbon in the way of functional groups of carbon–sulfur, carbon–oxygen, carbon–nitrogen, and carbon–halogen. In numerous books and review papers [51–58], the properties, and nature of those surface groups had been extensively examined.

Even though the inorganics from an aqueous phase can be adsorbed by all these surface groups, the surface groups of carbon–oxygen are the most prominent and influencing. The quantity of such carbon–oxygen surface functional groups can also be meaningfully increased by oxidation of carbon surface with hydrogen peroxide, ammonium persulfate, sodium hypochlorite, and nitric acid in aqueous media, besides oxygen or air in the gaseous phase at temperatures of 300°C–400°C. These oxidative treatments contain two kinds of surface carbon–oxygen groups, one neutral and the other acidic. The surface acid groups are polar and improve the charcoal ion exchanges and thus increase the cation sorption. Oxidized active carbons are of growing interest in extracting trace quantities of heavy metals from wastewater, in drinking water treatment, in silver and gold recovery and for purifying inorganic solutions. For instance, Linstedt et al. [59], Cheremisinoff [60] found in their experimental investigation that active carbon has a potential sorption power for removing metal ions from aqueous-solid solution. Also, Faust and Aly [61] and Cheremisinoff and Ellerbusch [62] examined the removal capacity on numerous cations for example selenium, vanadium, iron, barium and several fluorine, chlorine, and cyanide. Also, active carbon has also been utilized for the removal of cyanides, chlorates, chlorites, chlorides, nitrates, sulfides, borates, borax, boric acid, including certain metals from the aqueous phase such as dysprosium, strontium, iron, cerium, and lithium.

Ahmad et al. [63] researched the sorption of the Zn^{2+}, Pb^{2+}, and Cu^{2+} ions at 20°C on oxidized anthracite from aqueous-solid solutions. The uptake of metal ions improved with the solution having increased pH. The sorption process of mixed metal ions was reduced at an equivalent concentration. Yet, the overall sorption of metals was slightly higher than that of the single ion. Sorption based on the porous and chemical characteristics of the activated carbon surface was clarified. In addition, Ahmad et al. [63] found that the aqueous solution pH greatly affected the sorption equilibrium by active carbon produced from *Eucalyptus camaldulensis*. While the sorption of Zn^{2+} and Cu^{2+} cations below pH = 4.0 was negligible, those for Cr^{2+} was optimum at pH 2. Mathur et al. [64] have researched the sorption of several metals from wastewater by sorption on furnace slag and fly ash. Bituminous South African coal handled with bases [65] achieved nearly 99% elimination of metal ions from industrial wastewater [66]. Tiwari et al. [67] examined the adsorption of Ni^{2+}, Cu^{2+}, Cr(VI), and ions from diluted solutions in the 5–50 mg/L concentration range by sorption of activated carbon in the 5.5–8.0 pH range. The adsorption of Cu^{2+} showed a peak at pH = 8.0 and Cr(VI) at pH 5.5, while the sorption of nickel ions was significant in basic and acidic pH. The rate of Ni^{2+} sorption in the alkaline solution was faster. Jankowska et al. [68] found that oxidizing activated carbon at 420°C have increased copper and chromium sorption efficiency.

The sorption of Cr(VI) and Cr(III) from water solutions was also studied on various forms of activated carbons [69–73], such as on bituminous coal and fly ash [74]. These researchers noted a large sorption quantity of both Cr(III) and Cr(VI). However, the solution's sorption was dependent on the pH. All Cr(VI) sorption happened when the pH was acidic. Different carbon sorption efficiency varied from 99% to 30%.

The sorption of Cd^{2+} ions on the various active carbons and the effect of solvent pH were investigated by Youssef et al. [75]. With a rise of pH to 8.0 and adding of chelating agents, the amount of Cd^{2+} adsorbed increased. Cadmium adsorbed by normal carbons was greater than the acidic one. Dobrowolski et al. [76] found that the degree of the sorption of Cd^{2+} ions was dependent on the existence of carbon–oxygen surface groups.

Cu(II) sorption improved when the ionic concentration of the solution was improved with the addition of NaCl [77]. There were also studies on sorption of Cu(II) ions with effects with factors included pH and contact time as well as the solution concentration in the range from 10 to 1,000 mg/L [78,79].

3.4. Langmuir isotherm and the monolayer sorption capacity

Langmuir isotherms (C_e/q_e vs. C_e) from the experimental data in section 3.3 (sorption isotherm) are plotted in Fig. 4.

The plotting's equations and the corresponding calculated parameters of Langmuir isotherms are presented in Tables 3 and 4, respectively.

The linearity for all metal ions at both temperatures were satisfied (R^2 = 0.92–0.99). In some data, the lower correlation may also be known as a limiting factor for the Langmuir isotherm's applicability to describe behavior in the inhomogeneous surface where multi-layer sorption may possibly occur. For certain cases, the adsorbent's surface roughness is not taken into account. Inhomogeneous and irregular surfaces have several sorption sites with particular parameters, comprising heat of sorption, which vary from one location to another [32].

For all metals, the Langmuir constants (b) were between 0.012–0.125 (L/mg). The maximum monolayer sorption capacity Q_m at (298 and 313 K) were (≈47 and 58 mg/g) for Cu^{2+}, (≈45 and 44 mg/g) for Cd^{2+}, and (≈29 and 26 mg/g)

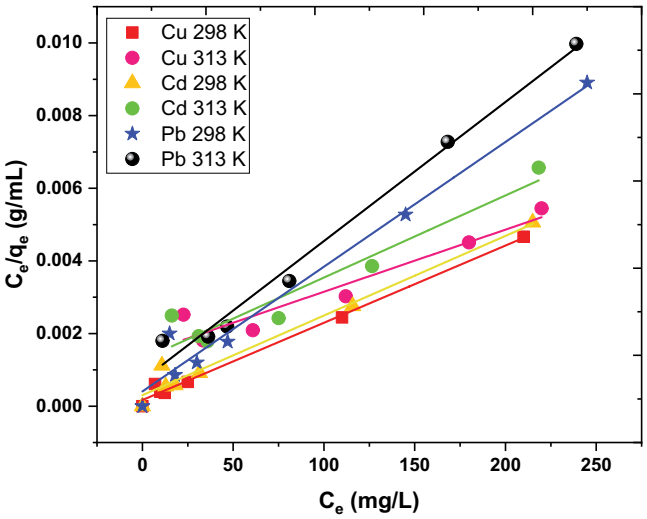

Fig. 4. Langmuir isotherms for Cu^{2+}, Cd^{2+}, and Pb^{2+} at 298 and 313 K.

Table 3
Plotting's equations of Langmuir isotherms for Cu^{2+}, Cd^{2+}, and Pb^{2+} at 298 and 313 K

Metal ions	Equation		R^2	
	298 K	313 K	298 K	313 K
Cu(II)	y = 2.126E-05x + 1.699E-04	y = 1.710E-05x + 1.441E-03	0.99	0.92
Cd(II)	y = 2.193E-05x + 3.027E-04	y = 2.261E-05x + 1.281E-03	0.98	0.92
Pb(II)	y = 3.434E-05x + 4.059E-04	y = 3.829E-05x + 7.180E-04	0.97	0.99

Table 4
Langmuir isotherms parameters for Cu^{2+}, Cd^{2+}, and Pb^{2+} at 298 and 313 K

Metal ions	Q_m (mg/g)		b (L/mg)		R_L	
	298 K	313 K	298 K	313 K	298 K	313 K
Cu(II)	47.030	58.482	0.125	0.012	0.093	0.468
Cd(II)	45.604	44.234	0.072	0.018	0.147	0.383
Pb(II)	29.118	26.117	0.085	0.053	0.129	0.186

for Pb^{2+}. The sorption capacities were enhanced at a lower temperature. The separation factor R_L for all metals is less than 1 indicating favorable sorption.

The amount adsorbed q_e was theoretically calculated (Figs. 5a–c) from the nonlinear Eq. (6) of Langmuir after entering the known values of b, Q_m, and (C_e = 0.1, 1, 2, etc.). The experimental data of all metals were fitted well by the theoretical lines. This indicates that the Langmuir isotherm was valid for the simulation of experimental results.

The literature review shows that activated carbon from several sources have been prepared and used to remove heavy metals (Table 5). A closer look at the literature on the use of Indian Almond, however, reveals a number of gaps and shortcomings in its use to remove Cu^{2+}, Cd^{2+}, and Pb^{2+}.

The surface of activated carbon has (C=C) bonds, which can add oxygen when the surface is oxidized and develop the surface groups of carbon–oxygen. Acidic and non-acidic are two kinds of surface oxygen groups. Acidic surfaces are polar in nature and are hypothesized as carboxyles and lactones, the classes of non-acid are known as quionones. The acidic surface groups are ionized and H^+ ions are formed when an oxidized active carbon is put into the aqueous solution [30].

$$C–COOH \rightarrow H^+ + C–COO^- \quad (A)$$

The proton (H^+) ions go toward the aqueous solution, which leaves the activated carbon surface sites with negative charge ($C–COO^-$). These negative sites create competition on the carbon surface between the heavy metal ions solution and the H^+ ions. With the availability, concentration, and oxidation of the activated carbon, the sorption of heavy metal ions on the oxidized carbon is increased at those negatively charged sites. These acidic oxygen groups are steadily removed from the carbon surface when the degassing takes place at rising temperatures. The site's surface ($>COO^-$) concentration decreases and consequently the sorption of heavy metal ions decreases in this way. The surface of carbon misplaces its negative character and can also get positively charged as the groups of oxygen are eliminated virtually entirely as degassed at 950°C, meaning that the repulsive relations between heavy metal ions and the carbon surface and become more prominent, resulting in a decline in ions sorption. For instance, when carbon is degassed at a temperature about 950°C and pH is higher than 7, the probability of copper precipitation as $Cu(OH)_2$ is improved. The sorption of Cu(II) ions in the carbon surface can also decrease [30].

The sorption rates increased in the following order $Cu^{2+} > Cd^{2+} > Pb^{2+}$ at a given equilibrium concentration. The theories were often based on ionic radii. In aqueous solutions, these cations will have the radii of $Cu^{2+}_{(aqueous)}$ = 0.419 nm, $Cd^{2+}_{(aqueous)}$ = 0.426 nm, and $Pb^{2+}_{(aqueous)}$ = 0.401 [87]. The Cu^{2+} ions would be more available than certain cations to other pores, including Cd^{2+} and Pb^{2+}, resulting in the improved sorption of Cu^{2+} ions. Pb^{2+} ions sorption could be less than the Cd^{2+} ions because of its lower polarizing strength such that the interactions between lead and carbon are weaker than the interactions between cadmium and carbon. The Cd(II) ions should only be adsorbed in areas in which the negative charging rate was more than adequate to retain Pb(II). The ionization of the acidic surface oxygen groups is responsible for the negative charges on carbon surfaces at elevated values of pH (>pH = ZPC). However, the amount of precisely sorbed ions on the solid surface does not only depends on the radii of the hydrated ions but also depends heavily on the metal electronegativity, the electron charge, the hydrolysis constant, etc.

The explanation of the system of activated carbon solutions allows it possible to understand the processes of the sorption of metals by activated carbons from aqueous solutions. If the acidic surface oxygen groups in the solution are ionized to produce H^+ ions on the activated carbon surface, the ionization degree depends on the pH of the solution [30]. With pH levels greater than ZPC the degree of ionization is very small and very strong where the solution pH reaches ZPC. Fig. 6 shows this ionization.

Table 5
Sorption capacity for some heavy metals into different adsorbents

Adsorbent	Sorption capacity (Q_m, mg/g)	References
Clinoptilolite (natural zeolite)	Cu^{2+} (3.37) Zn^{2+} (5.38) Mn^{2+} (2.42) Fe^{2+} (6.61)	[80]
Orange and banana peels	Cu^{2+} (4.75) Zn^{2+} (5.80) Pb^{2+} (7.97) Ni^{2+} (6.88) Co^{2+} (2.55)	[81]
Sesame straw biochar	Cu^{2+} (40.23) Zn^{2+} (34.71) Pb^{2+} (102.12) Cd^{2+} (86.03) Cr^{2+} (65.32)	[2]
Peanut husks	Cd^{2+} (50.58) Zn^{2+} (13.08) Ni^{2+} (16.43) Pb^{2+} (113.96)	[82]
Walnut sawdust	Pb^{2+} (15.90) Cd^{2+} (5.76) Ni^{2+} (3.29)	[83]
Wood sawdust	Cu^{2+} (6.88) Cd^{2+} (0.16) Zn^{2+} (0.97) Pb^{2+} (19.52)	[84]
Clay and coffee waste	Cd^{2+} (39.51) Ni^{2+} (11.03) Zn^{2+} (13.48)	[85]
Fruit shell of Indian almond	Cu^{2+} (31.21) Hg^{2+} (94.43)	[86]
Leaf samples of Indian almond	Cu^{2+} (45.03) Cd^{2+} (42.51) Pb^{2+} (27.57)	This study represented by the highest sorption capacity at lowest temperature.

The carbon surface sites are left negatively charged after the H^+ ions driven towards the aqueous phase. It results in electrostatic attractiveness amongst the sites that are charged negatively and the metal cations that are charged positively. When an oxidative treatment is given to the activated carbon surface, the number of negatively charged sites and hence the amount of acidic surface groups increases, leading to an increase in metal cation sorption due to attractive interactions. Likewise, as these surface acidic groups are eliminated by degassing from the carbon surface, the attractive electrostatic interactions as well as the sorption decrease depending on the reduction of the amount of acid groups removed from the surface of the carbon. Bansal et al. [88–90] performed comparative analyses on the adsorption of many metal cations on various granular and fibrous activated carbons by slowly strengthening and minimizing the quantity of acid carbon–oxygen surface functional groups. These researchers as well found a linear relation between the surface acidity of the carbon and the sorption of the amount of metal ion. In the issue of heat-treated carbons, Biniak et al. [91] through examining the Cu^{2+} sorption proposed that the process could include dipole/dipole interactions (p–d) between ionic metal species and the graphene layers.

3.5. Freundlich, Temkin, and Dubinin–Radushkevich isotherms and the multilayer sorption

Although Langmuir isotherm was well-fitted to the experimental results, multilayer sorption and interaction may likely be expected in the layer. Fig. 7 represents Freundlich, Temkin, and Dubinin–Radushkevich isotherms. In Table 6, the correlation coefficient (R^2) in Freundlich and Temkin isotherm was low especially at lower temperatures. However,

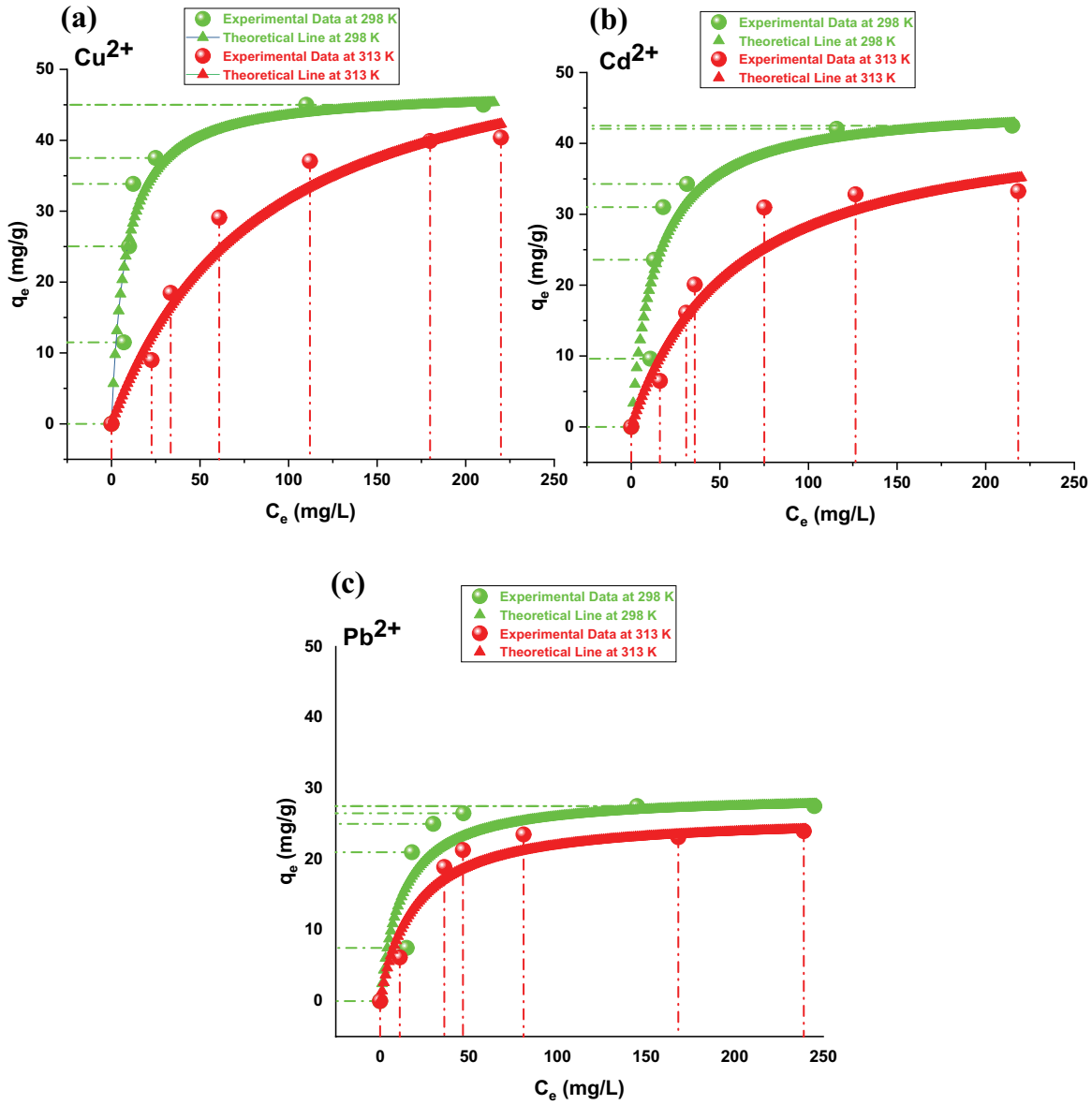

Fig. 5. Experimental and theoretical sorption isotherms for (a) Cu^{2+}, (b) Cd^{2+}, and (c) Pb^{2+} at 298 and 313 K.

the Dubinin–Radushkevich isotherms showed a strong linearity correlation and the q_s (mg/g) values were nearly similar to the q_e (mg/g) values obtained by the Langmuir isotherm.

3.6. Thermodynamic parameters from the constant (b) of Langmuir isotherm

The constant of Langmuir isotherm b (L/mg) was commonly used to derive the sorption capacity and parameters of thermodynamic in some studies [92–94]. The K_{aeq} (apparent equilibrium constant) that is very essential in calculating the thermodynamic parameters is unitless and is numerically equal to the Langmuir constant b. The C_r is the molar concentration of sorbate (mol/L).

$$K_{aeq} = bC_r \tag{17}$$

This remark agrees with Liu's [92] work. So, for the molar concentration of solute (mol/L), the above consideration seems reasonable. However, for common Langmuir isotherm studies, the adsorbate amounts were reported in mg/L, and the capacity of sorption was reported in mg/g. Several studies [93,94], have reviewed a suitable equation after discussions on several erroneous approaches that were adopted in the literature for the calculation of thermodynamic parameters from Langmuir isotherm.

Therefore, to transfer b (L/mg) in Langmuir to dimensionless, that is, to K_{aeq}, the following Eq. (18) is used for the dilute ionic solution or non-ionic solute:

$$K_{aeq} = bM_A \tag{18}$$

where M_A is assumed to be the atomic weight of adsorbate in mg/mole (i.e., atomic weight must be multiplied

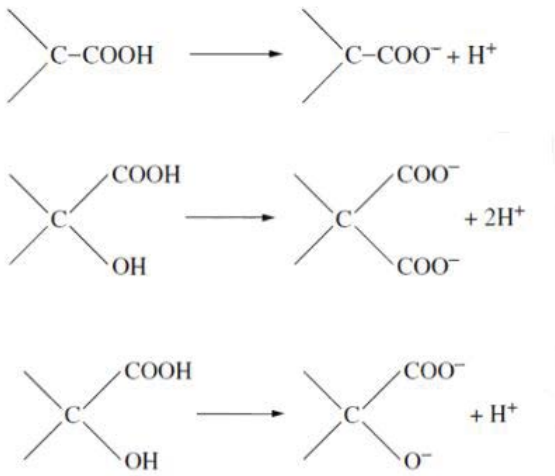

Fig. 6. Ionization on activated carbon surface [30].

by 1,000 and then by the Langmuir isotherm (b) to get the dimensionless K_{aeq}).

Eq. (19) of van't Hoff in aqueous-solid interface in the light of Langmuir isotherm (b) and for ionic and non-ionic solute in a dilute solution can be written as follows:

$$\ln bM_A = -\frac{\Delta H^\circ}{RT} + \frac{\Delta S^\circ}{R} \tag{19}$$

The ΔH° and ΔS° can be obtained by:

- plotting $\ln bM_A$ (i.e., $\ln K_{aeq}$) against $1/T$ based on Eq. (19).
- plotting ΔG° against T based on Eq. (13).

The ΔG° at the two temperatures (298 and 313 K) can be calculated from Eqs. (13) or (14). All these calculation methods gave the same results for (ΔH°, ΔS°, and ΔG°), see Fig. 8 and Table 7.

The ΔS° and ΔH° are temperature independent. The negative number of ΔH° represents the exothermic reaction while the positive one represents the endothermic reaction. The attraction between the sorbate and the sorbent is indicated by the positive number of ΔS°. As a result, the randomness of the solid–liquid interface increased, the flexibility of the sorbate increased, and the sorption process enhanced. Negative ΔS°, however, includes a less active interface of the liquid–solid system that causes sorption to be reduced [95]. The process of sorption is considered spontaneous When the ΔG° value is negative and the opposite is correct for a non-spontaneous process that occurred when ΔG° value is positive. Also, the thermodynamic efficiency of a reaction essentially depends on ΔG°. In delineating the sorption mechanism, the correct estimate of the thermodynamic parameter is crucial [93].

4. Conclusion

This research investigated the sorption of metal ions (Cu^{2+}, Cd^{2+}, and Pb^{2+}) from a synthetic solution onto the surface of activated carbon (prepared from *T. catappa* leaf samples). The Langmuir sorption isotherm demonstrated the relation between the adsorbed amount on the surface (q_e) and the remained amount or concentration in the solution (C_e). The experimental adsorbed amount (q_e) for Cu^{2+}, Cd^{2+}, and Pb^{2+} at (298 and 313 K) reached (45.0 and 40.4 mg/g), (42.5 and 33.2 mg/g) and (27.5 and 24.0 mg/g), respectively. Thus, under comparable conditions, the ability of sorption increases in the order $Cu^{2+} > Cd^{2+} > Pb^{2+}$.

Table 6
Freundlich, Temkin, and Dubinin–Radushkevich isotherms parameters for Cu^{2+}, Cd^{2+}, and Pb^{2+} at 298 and 313 K

Isotherm models	Cu^{2+}		Cd^{2+}		Pb^{2+}	
	298 K	313 K	298 K	313 K	298 K	313 K
Freundlich isotherm						
$1/n$	0.29	0.60	0.34	0.59	0.29	0.40
n	3.48	1.67	2.93	1.71	3.47	2.51
K_F (mg/g)	11.52	1.92	8.13	1.89	6.75	3.43
R^2	0.59	0.85	0.57	0.80	0.41	0.71
Temkin isotherm						
A_T (L/g)	2.13	0.11	1.09	6.56	2.05	1.67
b_T	307.54	190.74	282.64	243.29	507.10	483.75
B	8.06	13.64	8.77	10.70	4.89	5.38
R^2	0.75	0.95	0.75	0.90	0.51	0.78
Dubinin–Radushkevich isotherm						
q_s (mg/g)	46.09	39.15	44.27	31.19	30.25	23.24
K_{ad} (mol²/kJ²)	1.00E-05	1.00E-04	3.00E-05	7.00E-05	4.00E-05	3.00E-05
E (kJ/mol)	0.05	0.09	0.06	0.08	0.07	0.07
R^2	0.97	0.99	0.89	0.96	0.79	0.99

Table 7
Thermodynamic parameters for heavy metal ions calculated from Langmuir isotherm constant

Metal ions	b (L/mg)		K_{aeq}		ΔG° (kJ/mol)		ΔH° (kJ/mol)	ΔS° (J/K mol)
	298 K	313 K	298 K	313 K	298 K	313 K		
Cu(II)	0.125	0.012	7,952.060	754.191	–22.252	–17.242	–121.775	–0.334
Cd(II)	0.072	0.018	8,142.947	1,984.015	–22.310	–19.759	–73.000	–0.170
Pb(II)	0.085	0.053	17,532.738	11,049.983	–24.210	–24.228	–23.866	0.001

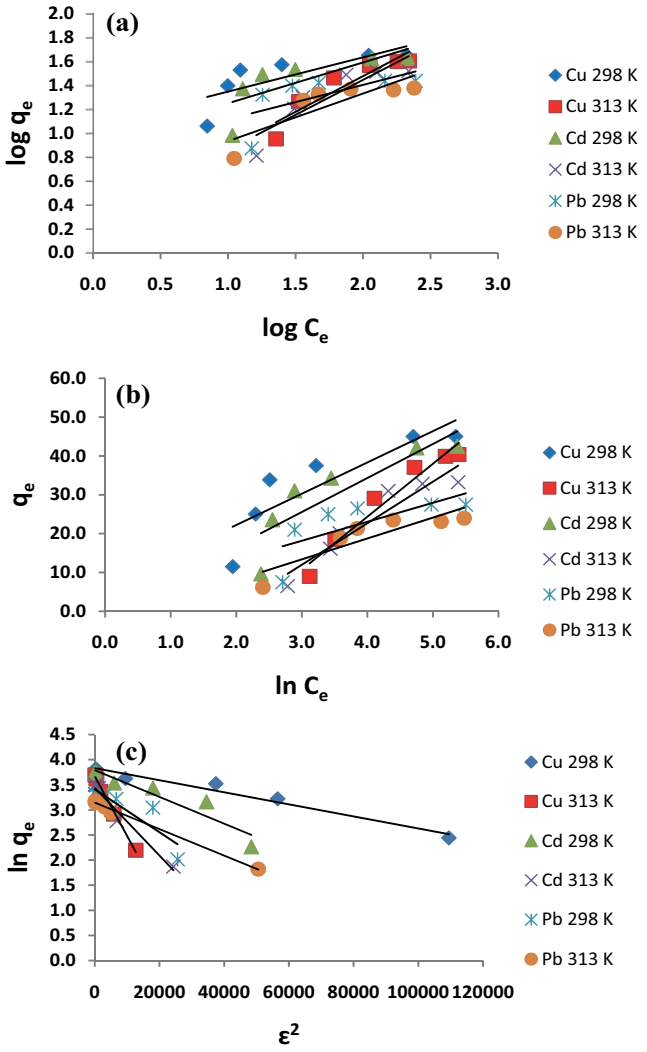

Fig. 7. (a) Freundlich, (b) Temkin, and (c) Dubinin–Radushkevich isotherms for Cu^{2+}, Cd^{2+}, and Pb^{2+} at 298 and 313 K.

The maximum monolayer sorption capacity Q_m at (298 and 313 K) was found to be (≈47 and 58 mg/g) for Cu^{2+}, (≈45 and 44 mg/g) for Cd^{2+}, and (≈29 and 26 mg/g) for Pb^{2+}. The sorption capacities were enhanced at lower temperatures. The separation factor R_L for all metals is less than 1 indicating favorable sorption. The experimental data of all metals were fitted well by the theoretical lines. This indicates that the Langmuir isotherm was valid for the simulation of experimental results.

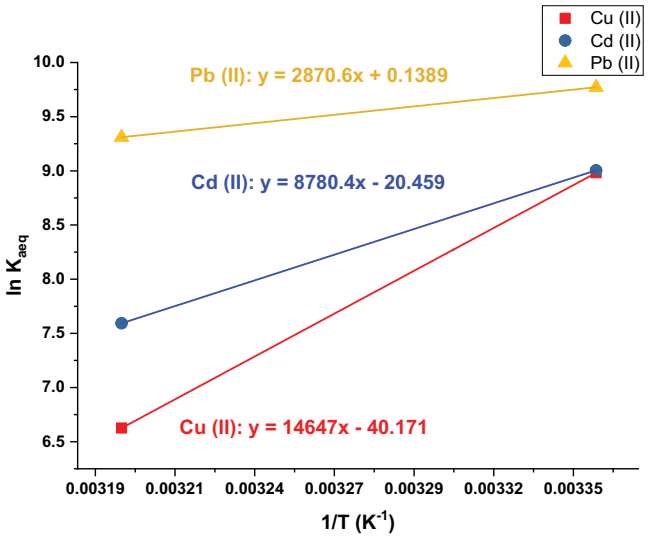

Fig. 8. Plot of lnK_{aeq} against 1/T for heavy metal ions.

Thermodynamic parameters for heavy metal ions using Langmuir isotherm constants were calculated. All values of (ΔH°, ΔG°, and ΔS°) were negative except the positive value of ΔS° in Pb^{2+}. The ΔS° and ΔH° are temperature independent. The negative numbers of ΔH° exemplify exothermic reaction. Negative ΔS°, however, includes a less active interface of the liquid–solid system that causes sorption to be reduced. The negative value of ΔG° indicates that the sorption is a spontaneous process. The activated carbon prepared from *T. catappa* leaf samples seemed to be beneficial in removing trace metals from environmental aqueous solutions.

Author contributions

Bandar designed the experiments; completed the experiments; evaluate the data; contributed chemicals/materials/laboratory analysis apparatuses and authored the article.

Funding

No external funding was given for this research.

Conflicts of interest

No conflicts of interest are declared by the author.

References

[1] S. Xu, Y. Liu, Y. Yu, X. Zhang, J. Zhang, Y. Li, PAN/PVDF chelating membrane for simultaneous removal of heavy

metal and organic pollutants from mimic industrial wastewater, Sep. Purif. Technol., 235 (2020) 2–9, doi: 10.1016/j.seppur.2019.116185.
[2] J.H. Park, Y.S. Ok, S.H. Kim, J.S. Cho, J.S. Heo, R.D. Delaune, D.C. Seo, Competitive adsorption of heavy metals onto sesame straw biochar in aqueous solutions, Chemosphere, 142 (2016) 77–83.
[3] V.K. Gupta, M. Al Khayat, A.K. Singh, M.K. Pal, Nano level detection of Cd(II) using poly(vinyl chloride) based membranes of Schiff bases, Anal. Chim. Acta, 634 (2009) 36–43.
[4] N. Madima, S.B. Mishra, I. Inamuddin, A.K. Mishra, Carbon-based nanomaterials for remediation of organic and inorganic pollutants from wastewater. A review, Environ. Chem. Lett., 18 (2020) 1169–1191.
[5] J. Lehmann, S. Joseph, S. Joseph, Biochar for Environmental Management, 2nd ed., Taylor & Francis, London, 2015.
[6] EBC (2012) 'European Biochar Certificate - Guidelines for a Sustainable Production of Biochar', European Biochar Foundation (EBC), Version 61, Arbaz, Switzerland, 2015, pp. 1–22.
[7] H. Marsh, F. Rodríguez-Reinoso, Activated Carbon, Elsevier Ltd., Amsterdam, The Netherlands, 2006.
[8] M. Smisek, S. Cerny, Activated Carbon, In: Topics in Organic and General Chemistry, Elsevier Co., New York, USA, 1970, pp. 93–123.
[9] I. Hilber, T.D. Bucheli, Activated carbon amendment to remediate contaminated sediments and soils: a review, Global Nest J., 12 (2010) 305–317.
[10] IBI, Standardized Product Definition and Product Testing Guidelines for Biochar That Is Used in Soil, International Biochar Initiative, 2015, 23 p. Available at: http://www.biochar-international.org/characterizationstandard (accessed July 24, 2020).
[11] N. Hagemann, K. Spokas, H.P. Schmidt, R. Kägi, M.A. Böhler, T.D. Bucheli, Activated carbon, biochar and charcoal: linkages and synergies across pyrogenic carbon's ABCs, Water (Switzerland), 10 (2018) 6–19, doi: 10.3390/w10020182.
[12] J.J. Schanz, R.H. Parry, The activated carbon industry, Ind. Eng. Chem., 54 (1962) 24–28.
[13] R.A. Smith, On the absorption of gases by charcoal. —No. I, Proc. R. Soc. London, 12 (1863) 424–426.
[14] J. Dewar, Absorption and thermal evolution of gases occluded in charcoal at low temperatures, Am. J. Sci., 4–18 (1904) 295–300.
[15] N. Chaney, The activation of carbon, Trans. Am. Electron. Chem Soc., 91 (1919) 3–6. Available at: https://scholar.google.com/scholar?hl=en&as_sdt=0%2C5&q=Chaney%2C+N.+The+activation+of+carbon.+Trans.+Am.+Electron.+Chem.+Soc.+3_6+1919%2C+91&btnG= (accessed July 24, 2020).
[16] N.K. Chaney, Adsorptive Carbon and Process of Making the Same, U.S. Patent 1497543, 1924. Available at: https://patentimages.storage.googleapis.com/12/63/66/dc18fe04d33abc/US1497543.pdf (accessed July 24, 2020).
[17] Metalbank-Co., Zinc Chloride for Activating Charcoal, British Patent 238,889, 1924. Available at: https://patents.google.com/patent/CA1334192C/en (accessed July 24, 2020).
[18] Bayer, Manufacture of Active Charcoal by Briquetting Charcoal Fines and Chemicals under Pressure, British Patents 195,390, 1923. Available at: https://pubs.acs.org/doi/pdf/10.1021/ie50249a009?src=recsys
[19] E.R. Sutcliffe, Absorbent and decolorising carbons, J. Soc. Chem. Ind., 43 (1924) 635–637.
[20] W.K. Lewis, A.B. Metzner, Engineering, design, and process development section activation of carbons, Ind. Eng. Chem., 46 (1954) 849–858.
[21] W.A. Helbig, Activated carbon, J. Chem. Educ., 23 (1946) 98–102, doi: 10.1021/ed023p98.
[22] W.M. Wright, Oxidations on charcoal, Math. Proc. Cambridge Philos. Soc., 23 (1926) 187–190.
[23] H.H. Lowry, On the nature of active carbon, J. Phys. Chem., 34 (1930) 63–73.
[24] O. Ruff, G. Schmidt, Amorpher kohlenstoff und graphit, Z. Anorg. Allg. Chem., 148 (1925) 313–331.
[25] H.H. Sheldon, Charcoal activation, Phys. Rev., 16 (1920) 165–172.
[26] G. Mezohegyi, F.P. van der Zee, J. Font, A. Fortuny, A. Fabregat, Towards advanced aqueous dye removal processes: a short review on the versatile role of activated carbon, J. Environ. Manage., 102 (2012) 148–164.
[27] F. Zhao, N. Rahunen, J.R. Varcoe, A. Chandra, C. Avignone-Rossa, A.E. Thumser, R.C.T. Slade, Activated carbon cloth as anode for sulfate removal in a microbial fuel cell, Environ. Sci. Technol., 42 (2008) 4971–4976.
[28] EPA, Fact Sheet: Mercury and Air Toxics Standards for Power Plants, 2011, pp. 1–6. Available at: https://www.epa.gov/mats/cleaner-power-plants (accessed July 24, 2020).
[29] Grand-View-Research-Group, Activated Carbon Market Size, Share | Global Industry Report, 2019–2025, 2019. Available at: https://www.grandviewresearch.com/industry-analysis/activated-carbon-market (accessed July 24, 2020).
[30] R.C. Bansal, M. Goyal, Activated carbon adsorption, Taylor & Francis, London, 2005.
[31] D. Parajuli, H. Kawakita, K. Inoue, K. Ohto, K. Kajiyama, Persimmon peel gel for the selective recovery of gold, Hydrometallurgy, 87 (2007) 133–139.
[32] B.R.M. Alsehli, A simple approach for determining the maximum sorption capacity of chlorpropham from aqueous solution onto granular activated charcoal, Processes, 8 (2020) 1–16, doi: 10.3390/pr8040398.
[33] D. Duranoğlu, A.W. Trochimczuk, U. Beker, Kinetics and thermodynamics of hexavalent chromium adsorption onto activated carbon derived from acrylonitrile-divinylbenzene copolymer, Chem. Eng. J., 187 (2012) 193–202.
[34] A.A. Khan, R.P. Singh, Adsorption thermodynamics of carbofuran on Sn(IV) arsenosilicate in H^+, Na^+ and Ca^{2+} forms, Colloids Surf., 24 (1987) 33–42.
[35] J.W. Biggar, M.W. Cheung, Adsorption of picloram(4-amino-3,5,6-trichloropicolinic acid) on panoche, ephrata, and palouse soils: a thermodynamic approach to the adsorption mechanism, Soil Sci. Soc. Am. J., 37 (1973) 863–868.
[36] W. Huang, J. Chen, F. He, J. Tang, D. Li, Y. Zhu, Y. Zhang, Effective phosphate adsorption by Zr/Al-pillared montmorillonite: insight into equilibrium, kinetics and thermodynamics, Appl. Clay Sci., 104 (2015) 252–260.
[37] M.F. Sawalha, J.R. Peralta-Videa, J. Romero-González, J.L. Gardea-Torresdey, Biosorption of Cd(II), Cr(III), and Cr(VI) by saltbush (*Atriplex canescens*) biomass: thermodynamic and isotherm studies, J. Colloid Interface Sci., 300 (2006) 100–104.
[38] S. Mandal, S. Tripathy, T. Padhi, M.K. Sahu, R.K. Patel, Removal efficiency of fluoride by novel Mg-Cr-Cl layered double hydroxide by batch process from water, J. Environ. Sci., 25 (2013) 993–1000.
[39] S. Kundu, A.K. Gupta, Investigations on the adsorption efficiency of iron oxide coated cement (IOCC) towards As(V)—kinetics, equilibrium and thermodynamic studies, Colloids Surf., A, 273 (2006) 121–128.
[40] S. Dawood, T.K. Sen, Removal of anionic dye Congo red from aqueous solution by raw pine and acid-treated pine cone powder as adsorbent: equilibrium, thermodynamic, kinetics, mechanism and process design, Water Res., 46 (2012) 1933–1946.
[41] L. Batistella, L.D. Venquiaruto, M. Di Luccio, J.V. Oliveira, S.B.C. Pergher, M.A. Mazutti, D. de Oliveira, A.J. Mossi, H. Treichel, R. Dallago, Evaluation of acid activation under the adsorption capacity of double layered hydroxides of Mg–Al–CO_3 type for fluoride removal from aqueous medium, Ind. Eng. Chem. Res., 50 (2011) 6871–6876.
[42] Q. Chang, L. Zhu, Z. Luo, M. Lei, S. Zhang, H. Tang, Sono-assisted preparation of magnetic magnesium–aluminum layered double hydroxides and their application for removing fluoride, Ultrason. Sonochem., 18 (2011) 553–561.
[43] D.P. Das, J. Das, K. Parida, Physicochemical characterization and adsorption behavior of calcined Zn/Al hydrotalcite-like compound (HTlc) towards removal of fluoride from aqueous solution, J. Colloid Interface Sci., 261 (2003) 213–220.
[44] L. Lv, Defluoridation of drinking water by calcined Mg-Al-CO_3 layered double hydroxides, Desalination, 208 (2007) 125–133.

[45] W. Ma, N. Zhao, G. Yang, L. Tian, R. Wang, Removal of fluoride ions from aqueous solution by the calcination product of Mg–Al–Fe hydrotalcite-like compound, Desalination, 268 (2011) 20–26.
[46] R. Chang, Physical Chemistry for the Chemical and Biological Sciences, University Science Books, Sausalito-USA, 2001.
[47] R. Chakraborty, A. Asthana, A.K. Singh, B. Jain, A.B.H. Susan, Adsorption of heavy metal ions by various low-cost adsorbents: a review, Int. J. Environ. Anal. Chem., 100 (2020) 1–38, doi: 10.1080/03067319.2020.1722811.
[48] J. Biscoe, B.E. Warren, An X-ray study of carbon black, J. Appl. Phys., 13 (1942) 364–371.
[49] Y.S. Ho, Citation review of Lagergren kinetic rate equation on adsorption reactions, Scientometrics, 59 (2004) 171–177.
[50] Y.S. Ho, G. McKay, Sorption of dye from aqueous solution by peat, Chem. Eng. J., 70 (1998) 115–124.
[51] H.P. Boehm, Some aspects of the surface chemistry of carbon blacks and other carbons, Carbon, 32 (1994) 759–769.
[52] H.P. Boehm, Chemical identification of surface groups, Adv. Catal., 16 (1966) 179–274.
[53] J.W. Patrick, Active carbon, Chem. Eng. J., 40 (1989) 196–197.
[54] W.S. Stoy, M.D. Garret, CARBON BLACK, Pigment, Pt 1 12 (1975) 261–304, doi: 10.1016/b978-0-08-009421-2.50013-5.
[55] J.S. Mattson, H.B. Mark, Activated Carbon, Marcel Dekker, New York, NY, 1971.
[56] H. Jankowska, A. Swiatkowski, J. Choma, Active Carbon, Ellis Horwood, West Sussex, 1991.
[57] K. Kinoshita, Carbon: Electrochemical and Physicochemical Properties, John Wiley Sons,New York, NY, London, 1988. Available at: http://www.wiley.com/WileyCDA/WileyTitle/productCd-0471848026.html (accessed July 25, 2020).
[58] M. Smisek, S. Cerny, Active Carbon, Manufacture, Properties and Applications, In: Topics in Inorganic and General Chemistry, Elsevier Publishing Company, 1970. Available at: https://www.amazon.com/Active-Carbon-Manufacture-Properties-Applications/dp/0444407731 (accessed July 25, 2020).
[59] K.D. Linstedt, C.P. Houck, J.T. O'Connor, Trace element removals in advanced wastewater treatment processes., J. Water Pollut. Control Fed., 43 (1971) 1507–1513.
[60] P.N. Cheremisinoff, Y.H. Habib, Cadmium, lead, mercury: a plenary account for water pollution: removal techniques, Water Sewage Works, 7 (1972) 46–51.
[61] S.D. Faust, O.M. Aly, Chemistry of Water Treatment, 1998. Available at: https://books.google.com.sa/books?hl=en&lr=&id=ivLiNH-NjOcC&oi=fnd&pg=PA1&dq=Faust,+S.D.+and+Aly,+O.M.,+Chemistry+of+Water+Treatment,+Chelsia,+M.L.,+Ed.,+Ann+Arbor+Press,+1988&ots=MEAdfUTPgP&sig=R_kzephbZNEN2T8T3hBPBydJLzw&redir_esc=y#v=onepage&q&f=false (accessed July 25, 2020).
[62] P.N. Cheremisinoff, F. Ellerbusch, Carbon Adsorption Handbook, Ann Arbor Science Publishers, Ann Arbor, MI, 1978.
[63] T.W. Ahmad, T.H. Usmani, Z. Ahmad, Activated carbon from indigenous inferior woods part II. Activation temperature, time and particle size influence, Pak. J. Sci. Ind. Res., 33 (1990) 177–180. Available at: https://agris.fao.org/agris-search/search.do?recordID=PK19910001339 (accessed July 26, 2020).
[64] A. Mathur, S.K. Khare, D.C. Rupainwar, Removal of heavy metals from main sewer-water of Varanasi city by adsorption on fly ash and blast furnace slag, J. Ind. Pollut. Control., 5 (1989) 52–57. Available at: https://scholar.google.com/citations?hl=en&user=sXOu2DIAAAAJ&view_op=list_works&sortby=pubdate#d=gs_md_cita-d&u=%2Fcitations%3Fview_op%3Dview_citation%26hl%3Den%26user%3DsXOu2DIAAAAJ%26sortby%3Dpubdate%26citation_for_view%3DsXOu2DIAAAAJ%3AMXK_kJrjxJIC%26t (accessed July 26, 2020).
[65] E.M. van der Merwe, L.C. Prinsloo, C.L. Mathebula, H.C. Swart, E. Coetsee, F.J. Doucet, Surface and bulk characterization of an ultrafine South African coal fly ash with reference to polymer applications, Appl. Surf. Sci., 317 (2014) 73–83.
[66] U.I. Gaya, E. Otene, A.H. Abdullah, Adsorption of aqueous Cd(II) and Pb(II) on activated carbon nanopores prepared by chemical activation of doum palm shell, Springerplus, 4 (2015) 1–18.
[67] D.P. Tiwari, K. Promod, A.K. Mishra, R.P. Singh, R.P.S. Srivastav, Removal of toxic metals from electroplating industries (effect of pH on removal by adsorption), Indian J. Environ. Health, 31 (1989) 120–124.
[68] H. Jankowska, J. Choma, W. Burakiewiez-Mortka, A. Swiatkowski, Active Carbon, Ellis Horwood Ltd., London, 1987.
[69] R. Gottipati, G. Ecocarb, T. Rourkela, Application of response surface methodology for optimization of Cr(III) and Cr(VI) adsorption on commercial activated, Res. J. Chem. Sci., 2 (2012) 40–48. Available at: https://www.researchgate.net/publication/225076280 (accessed July 26, 2020).
[70] C.P. Huang, M.H. Wu, The removal of chromium(VI) from dilute aqueous solution by activated carbon, Water Res., 11 (1977) 673–679.
[71] I. Bautista-Toledo, J. Rivera-Utrilla, M.A. Ferro-García, C. Moreno-Castilla, Influence of the oxygen surface complexes of activated carbons on the adsorption of chromium ions from aqueous solutions: effect of sodium chloride and humic acid, Carbon, 32 (1994) 93–100.
[72] G.G. Jayson, J.A. Sangster, G. Thompson, M.C. Wilkinson, Adsorption of chromium from aqueous solution onto activated charcoal cloth, Carbon, 31 (1993) 487–492.
[73] G.J. Alaerts, V. Jitjaturunt, P. Kelderman, Use of coconut shell-based activated carbon for chromium(VI) removal, Water Sci. Technol., 21 (1989) 1701–1704.
[74] D. Singh, N.S. Rawat, Sorption of Pb(II) by bituminous coal, Indian J. Chem. Technol., 2 (1995) 49–50. Available at: http://nopr.niscair.res.in/handle/123456789/31091 (accessed July 25, 2020).
[75] A.M. Youssef, T. El-Nabarawy, S.E. Samra, Sorption properties of chemically-activated carbons: 1. Sorption of cadmium(II) ions, Colloids Surf., A, 235 (2004) 153–163.
[76] R. Dobrowolski, M. Jaroniec, M. Kosmulski, Study of Cd(II) adsorption from aqueous solution on activated carbons, Carbon, 24 (1986) 15–20.
[77] L.S. de Lima, M.D.M. Araujo, S.P. Quináia, D.W. Migliorine, J.R. Garcia, Adsorption modeling of Cr, Cd and Cu on activated carbon of different origins by using fractional factorial design, Chem. Eng. J., 166 (2011) 881–889.
[78] M.A. Kahn, Y.I. Khattak, Adsorption of copper from copper sulfate solution on carbon black "Spheron 9"—II, Carbon, 30 (1992) 957–960.
[79] K.S. Low, C.K. Lee, S.L. Wong, Effect of dye modification on the sorption of copper by coconut husk, Environ. Technol., 16 (1995) 877–883.
[80] T. Motsi, N.A. Rowson, M.J.H. Simmons, Adsorption of heavy metals from acid mine drainage by natural zeolite, Int. J. Miner. Process., 92 (2009) 42–48.
[81] G. Annadurai, R.S. Juang, D.J. Lee, Adsorption of heavy metals from water using banana and orange peels, Water Sci. Technol., 47 (2003) 185–190.
[82] S. Ricordel, S. Taha, I. Cisse, G. Dorange, Heavy metals removal by adsorption onto peanut husks carbon: characterization, kinetic study and modeling, Sep. Purif. Technol., 24 (2001) 389–401.
[83] Y. Bulut, Z. Tez, Removal of heavy metals from aqueous solution by sawdust adsorption, J. Environ. Sci., 19 (2007) 160–166.
[84] M. Šćiban, B. Radetić, Ž. Kevrešan, M. Klašnja, Adsorption of heavy metals from electroplating wastewater by wood sawdust, Bioresour. Technol., 98 (2007) 402–409.
[85] V. Boonamnuayvitaya, C. Chaiya, W. Tanthapanichakoon, S. Jarudilokkul, Removal of heavy metals by adsorbent prepared from pyrolyzed coffee residues and clay, Sep. Purif. Technol., 35 (2004) 11–22.
[86] B.S. Inbaraj, N. Sulochana, Mercury adsorption on a carbon sorbent derived from fruit shell of *Terminalia catappa*, J. Hazard. Mater., 133 (2006) 283–290.

[87] E.R. Nightingale, Phenomenological theory of ion solvation. Effective radii of hydrated ions, J. Phys. Chem., 63 (1959) 1381–1387.
[88] M. Goyal, V.K. Rattan, D. Aggarwal, R.C. Bansal, Removal of copper from aqueous solutions by adsorption on activated carbons, Colloids Surf., A, 190 (2001) 229–238.
[89] M. Goyal, V.K. Rattan, R.C. Bansal, Adsorption of nickel from aqueous solutions by activated carbons, Indian J. Chem. Technol., 6 (1999) 305–312. Available at: http://nopr.niscair.res.in/handle/123456789/16961 (accessed July 24, 2020).
[90] R.C. Bansal, D. Aggarwal, M. Goyal, B.C. Kaistha, Influence of carbon-oxygen surface groups on the adsorption of phenol by activated carbons, Indian J. Chem. Technol., 9 (2002) 290–296. Available at: http://nopr.niscair.res.in/handle/123456789/18898 (accessed July 25, 2020).
[91] S. Biniak, A. Swiatkowski, M. Pakula, Electrochemical Studies of Phenomena at Active Carbon-Electrolyte Solution Interfaces, L.R. Radovic, Ed., Chemistry and Physics of Carbon, Marcel Dekker, New York, NY, 2001, pp. 125–225.
[92] Y. Liu, Is the free energy change of adsorption correctly calculated?, J. Chem. Eng. Data, 54 (2009) 1981–1985.
[93] P.S. Ghosal, A.K. Gupta, Determination of thermodynamic parameters from Langmuir isotherm constant-revisited, J. Mol. Liq., 225 (2017) 137–146.
[94] E.C. Lima, A. Hosseini-Bandegharaei, J.C. Moreno-Piraján, I. Anastopoulos, A critical review of the estimation of the thermodynamic parameters on adsorption equilibria. Wrong use of equilibrium constant in the Van't Hoof equation for calculation of thermodynamic parameters of adsorption, J. Mol. Liq., 273 (2019) 425–434.
[95] P. Saha, S. Chowdhury, Insight Into Adsorption Thermodynamics, M. Tadashi, Ed., Thermodynamics, INTECH Open Access Publisher, Janeza-Croatia, 2011. Available at: https://www.intechopen.com/books/thermodynamics/insight-into-adsorption-thermodynamics